ity to control the energy of the beam in time is not the simplest requirement on an electron-beam machine, but may be feasible through design of a multielement accelerator or decelerator downstream from the ordinary diode.[10]

A more fundamental limitation of this method concerns acceleration to velocities close to c. As mentioned above, there is a lag between introduction of a modulation and the time it reaches the particles, because of finite propagation speed. For $V_{ph} \gtrsim 0.5c$, one can imagine the waves almost outrunning the modulation. Of course, the "kick" from the modulation eventually does catch up, but the additional distance traversed by the particles in the interim has the effect of weakening the average accelerating field. For these high velocities, therefore, it may be more efficient to use other collective-acceleration schemes, some of which, in fact, are inefficient at low velocity.[11] In other applications, ion energies of 100–200 MeV may be acceptable as they are. Finally, even though high velocities may be inaccessible, the use of higher-atomic-number ions, such as in heavy-ion fusion, would still permit generation of significant ion energies, 10–20 GeV for $A = 200$, in very-modest-length accelerators.

There are still many unanswered questions concerning the effect of energy modulations on collective plasma effects. Preliminary studies indicate that the eigenmodes of the cyclotron waves are not seriously affected by this, but these matters require more detailed analytic and numerical studies. These studies are in progress, as well as studies into the effect of energy modulation on other beam modes.

We would like to thank Dr. B. S. Newberger for useful discussions on this subject.

[1]M. L. Sloan and W. E. Drummond, Phys. Rev. Lett. 31, 1234 (1973).
[2]P. Sprangle, W. M. Manheimer, and A. T. Drobot, Phys. Rev. Lett. 36, 1180 (1976).
[3]C. L. Olson, Phys. Rev. A 11, 2631 (1974).
[4]C. L. Olson, Part. Accel. 6, 197 (1975).
[5]S. Putnam, Phys. Rev. Lett. 25, 1129 (1970).
[6]A. V. Agafonov, A. A. Kolomenskii, and I. I. Logochev, Pis'ma Zh. Eksp. Teor. Fiz. 22, 478 (1975) [JETP Lett. 22, 231 (1975)].
[7]R. B. Miller, R. J. Faehl, T. C. Genoni, and W. A. Proctor, IEEE Trans. Nucl. Sci. 24, 1948 (1977).
[8]W. E. Drummond, G. I. Bourianoff, D. E. Hasti, W. W. Rienstra, M. L. Sloan, and J. R. Thompson, Air Force Weapons Laboratory Report No. AFWL-TR-74-343, 1975 (unpublished).
[9]D. C. Straw, private communication.
[10]A. I. Pavlovskii, V. S. Bosarnykin, G. D. Kuleshov, A. I. Gerasimov, V. A. Tananakin, and A. P. Klement'ev Dokl. Akad. Nauk SSSR 222, 817 (1975) [Sov. Phys. Dokl. 20, 441 (1975)].
[11]B. B. Godfrey, to be published.

Stabilization of Drift Waves by Lower-Hybrid Fields

R. Gore, J. Grun, and H. Lashinsky
Institute for Physical Science and Technology, University of Maryland, College Park, Maryland 20742
(Received 16 February 1978)

Stabilization of drift waves by external rf fields at frequencies near the lower-hybrid frequency has been observed experimentally in a Q machine in the collisionless regime with $(\omega_{pe}/\omega_{ce})^2 \ll 1$. Stabilization is due to a resonant ponderomotive force which increases the drift frequency, thus enhancing the electron Landau damping. The observations are in general accord with analyses in the literature when finite-geometry effects appropriate to the present experiment are taken into account.

The use of rf power at the lower-hybrid frequency has frequently been considered as a means of supplementary plasma heating for fusion purposes.[1] It is therefore of interest to examine the effect of lower-hybrid fields on low-frequency modes such as the drift instabilities, which are sometimes thought to play an undesirable role in experimental plasma devices.

In this Letter we present experimental results which indicate that the drift instability in a collisionless plasma can be stabilized by the application of rf fields near the lower-hybrid frequency. A novel feature of the work is the experimental demonstration of the effect of a *resonant* ponderomotive force which is amplified and changes sign when the frequency of the applied field is

equal to a characteristic plasma resonance frequency. The results described here are in general accord with analyses in the literature[2-5] when finite-geometry effects appropriate to the present experiment are taken into account.

The stabilization of the drift instability can be understood from the following qualitative physical picture.[6] Consider a plasma with an inhomogeneous transverse density distribution in a longitudinal magnetic field; in general such a plasma is unstable against a collisionless drift wave, say with frequency ω, wave number k, density perturbation n_ω, and electric field E_ω. A pump wave at frequency Ω ($\Omega \gg \omega$), with wave number K and electric field E_Ω, in the present case an electrostatic lower-hybrid wave, is excited in the plasma by external means and gives rise to an equilibrium in which the electrons execute oscillatory motion at frequency Ω with velocity V_Ω. Nonlinear coupling between the high-frequency velocity V_Ω and the low-frequency density perturbation n_ω leads to the production of sideband electrostatic fields E_+ and E_- characterized by frequencies and wave numbers $\omega+\Omega$, $k+K$ and $\omega-\Omega$, $k-K$, respectively. (Only lowest-order coupling is considered.) The sideband fields interact with the pump field to generate a ponderomotive force proportional to $\nabla\langle(E_\Omega+E_++E_-)^2\rangle$, which reduces to $\nabla\langle E_\Omega E_\pm\rangle$ when terms unimportant in the present context are neglected (the brackets denote high-frequency averages). This ponderomotive force adds to the thermal pressure associated with the drift wave, thus increasing the drift frequency (for fixed k), in which case the electron Landau damping becomes stronger than the pertinent destabilization mechanism.

The effect of a resonant ponderomotive force on a particle in an inhomogeneous high-frequency electric field can be understood from the basic definition of the ponderomotive force: $\vec{F}=e\langle(\vec{d}\cdot\nabla)\vec{E}(t,r)\rangle$, where e is the particle charge, $\vec{E}(t,r)$ is the high-frequency inhomogeneous electric field, $\vec{d}$ is the high-frequency particle displacement, and the brackets denote a high-frequency average. In the resonance case, the particle is subject to a restoring force and executes bounded oscillatory motion (such as the lower-hybrid oscillations in the present case) described by $\ddot{d}+\Omega_R^2 d=eE(t,r)/m$, where Ω_R is a characteristic resonance frequency and d becomes a resonant displacement that changes sign when the field frequency is equal to Ω_R, thus reversing the sign of the ponderomotive force. This sign change is a central feature of the experimental results described below.

The modification of the drift frequency caused by the ponderomotive force can be obtained from the analysis of Fainberg and Shapiro.[3] We consider a plasma with inhomogeneous density distribution $n(x)$ in a uniform magnetic field $B\hat{z}$, subject to a uniform electric field[7] $\vec{E}=E_0\hat{z}\cos\Omega t$, where $\Omega\approx\Omega_{\rm LH}$. For the present experimental conditions, in which $(\omega_{pe}/\omega_{ce})^2\ll 1$ and $(\omega_{pi}/\omega_{ci})^2\ll 1$, the lower-hybrid frequency is

$$\Omega_{\rm LH}=[(K_z/K)^2\omega_{pe}^2+\omega_{pi}^2]^{1/2}. \tag{1}$$

In the presence of the rf electric field the electrons oscillate with velocity $V_\Omega=(eE_0/m\Omega)\sin\Omega t$ and perturbations about this oscillatory equilibrium are written as the sum of a high-frequency component (Ω) and a low-frequency component (ω), where $\omega\approx\omega_*=(ck_\perp T_e/Be)(1/n)(dn/dx)$. The equation that describes the balance of low-frequency forces in the z direction is found to be

$$E_\omega+\frac{\nabla n_\omega}{en_0}\left[T_e+\frac{2\pi n_0 e^2 a^2}{k^2}\varphi(\Omega)\right]=0, \tag{2}$$

where n_0 is the zeroth-order density distribution, n_ω is the low-frequency density perturbation, E_ω is the low-frequency electric field, and $a=k_z eE_0/m\Omega^2$ is the ratio of the high-frequency electron excursion to the drift wavelength; the effect of the rf field appears in the second term in the rectangular bracket and the function $\varphi(\Omega)$ is given by

$$\varphi(\Omega)=\Omega^2\frac{(\Omega^2-\Omega_{\rm LH}^2)}{(\Omega^2-\Omega_{\rm LH}^2)^2-\Omega^2\omega_*^2/(k\lambda_D)^4}, \tag{3}$$

when $(\omega_{pe}/\omega_{ce})^2\ll 1$. Equation (2) is then used to obtain the drift-wave frequency in the presence of the rf field[3]:

$$\omega(\Omega)=-\omega_*[1+(1/2)(a/k\lambda_D)^2\varphi(\Omega)]. \tag{4}$$

It should be noted that the function $\varphi(\Omega)$ in Eq. (3) has two poles separated by a zero, as in Fig. 1(a). This function can be used to sketch the general behavior of the frequency $\omega(\Omega)$ in Eq. (4), as is done in Fig. 1(b), in which the singular behavior at the poles P_1 and P_2 has been "rounded off" to take account of effects that are not included in the idealized theory, but which are observed experimentally.

The stabilization mechanism of interest here can be interpreted in terms of the work done on the resonant electrons by the electric field of the drift wave, which is proportional to the negative

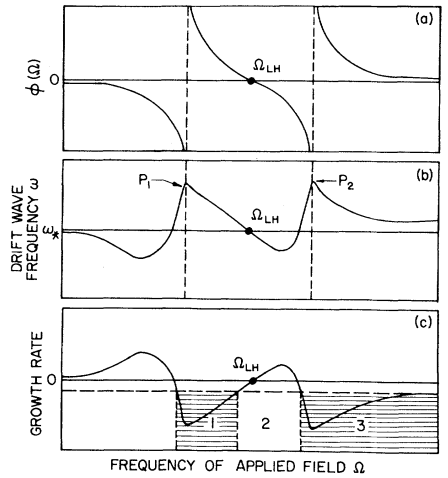

FIG. 1. (a) The resonance function $\varphi(\Omega)$ of Eq. (3), (b) dependence of drift-wave frequency ω on applied frequency Ω modified to take account of effects not included in the idealized theory, (c) the ponderomotive component of the growth rate for the drift wave as a function of the applied frequency Ω. The zero of the abcissa scale is suppressed in these figures so that the entire variation of applied frequency lies in the lower-hybrid region.

of the growth rate[8]:

$$dW/dt=(eE_z\omega/k_z)^2(f_0/T)[1-\omega_*/\omega], \qquad (5)$$

where f_0 is a Maxwellian velocity distribution and $dW/dt>0$ corresponds to stability. When $\omega=\omega_*$, Eq. (5) shows that $dW/dt=0$ (marginal stability), reflecting the well-known balance between the destabilizing effect of the density gradient and the stabilizing effect of the electron Landau damping.[8] Similarly, any mechanism that makes $\omega<\omega_*$ ($\omega>\omega_*$) causes growth (damping) of the drift wave. Thus, the function $\omega(\Omega)$ in Fig. 1(b) leads to the dependence of growth rate on Ω with alternating regions of growth and damping as shown by the curve in Fig. 1(c). In the present experiment (collisionless plasma with $\nabla T=0$ and finite ion Larmor radius, $\rho_i\neq 0$), with no rf electric field $\omega=\omega_*[1-(k_\perp\rho_i)^2]<\omega_*$ because the average low-frequency electric field seen by the ions is reduced by the finite-Larmor-radius effect, and the plasma is unstable.[8] Stabilization of the drift wave occurs when the damping due to the ponderomotive force becomes greater than some critical value that corresponds to the finite-Larmor-radius destabilization. This critical value of the damping is indicated by the horizontal dashed line in Fig. 1(c), and intersections of the growth curve with this line mark the boundaries of stabilization "windows" within which the drift wave is stabilized. These frequency windows are indicated by the horizontal cross hatching in the figure.

The experimental work described here has been carried out on the University of Maryland Q machine operated single-ended in the collisionless regime with $n=10^8$ cm^{-3}, $B=1.8$ kG, $T_e=0.2$ eV, plasma length $L=70$ cm, and plasma radius $r=2$ cm. For these values the parameter $(\omega_{pe}/\omega_{ce})^2=10^{-4}$, the electron-ion mean free path is greater than L, the Debye length $\lambda_D=3\times10^{-2}$ cm, and $k_\perp\rho_i\approx 0.1$. Radio-frequency power is coupled into the plasma by means of a short coil, inductive coupling being used since it provides an optimum match to the plasma with selective excitation of a single lower-hybrid mode. It should be emphasized that the coil excites discrete lower-hybrid modes characteristic of the bounded plasma column, and that the values of K_z and K in Eq. (1) "quantized" by the plasma geometry. Thus, the longitudinal rf electric field $E_\Omega=K_z\Phi$ (Φ is the electrostatic potential associated with the lower-hybrid mode) derives from the properties of the lower-hybrid mode; the amplitude with which this mode is excited depends on the geometry, position, and coupling efficiency of the coil. The frequencies, quality factors (Q), rf field configurations, and absorbed powers for these discrete modes have been determined in separate experiments, in which the various discrete lower-hybrid resonances are examined by measuring the frequency dependence of the Q of the coil with an accurate and sensitive commercial Q meter. This work is described elsewhere.[9,10]

In the present experiments the frequency $\omega/2\pi$ and amplitude of the drift wave are measured as the applied frequency $\Omega/2\pi$ is varied in the vicinity of the frequency $\Omega_{LH}/2\pi$, which corresponds to one of the lower-hybrid resonances. The rf power is kept fixed at a level which corresponds to $E^2/8\pi nkT=10^{-2}$ and $a=10^{-2}$. In other experiments it has been shown that with $\Omega=$ const the dependence of drift-wave frequency on pump-wave amplitude is in qualitative agreement with Eq. (4) over an order-of-magnitude variation in rf power, although more refined experiments will be required to determine this relation quantitatively. The frequency $\omega(\Omega)$ is conveniently presented in the form of a raster display[11] in which $\omega/2\pi$ is observed on a spectrum analyzer as $\Omega/2\pi$ is slowly swept through $\Omega_{LH}/2\pi$, with successive sweeps of the spectrum analyzer being stacked one above the other as shown in Fig. 2. Comparison between experiment and the analysis given above is

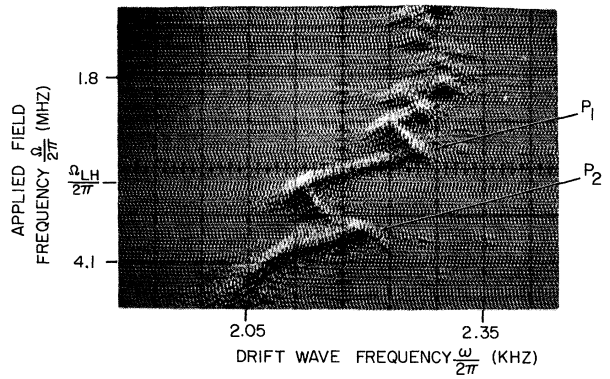

FIG. 2. The dependence of drift-wave frequency $\omega/2\pi$ on applied frequency $\Omega/2\pi$ as shown by a raster display (Ref. 11). In this display system successive sweeps of a spectrum analyzer are stacked one above the other. The points marked $P_1 = 2.6$ MHz and $P_2 = 3.7$ MHz are to be compared with similarly designated points in Fig. 1(b). The secular frequency shift is due to a variation in rf power coupled into plasma caused by the frequency dependence of the coil Q and by the distributed capacity of the coil.

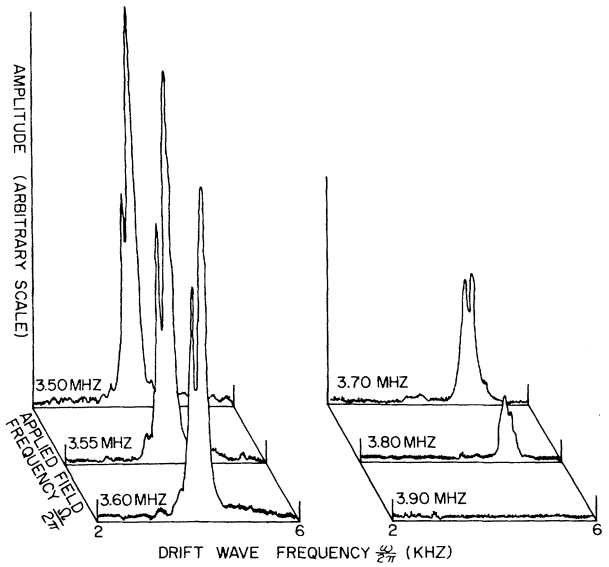

FIG. 3. The drift-wave amplitude as a function of the applied frequency in the neighborhood of the lower-hybrid frequency $\Omega_{LH}/2\pi$. Successive tracings have been displaced horizontally to avoid confusion. In this series $\Omega_{LH}/2\pi = 3.55$ MHz and the endpoints of the drift-wave frequency scale are nominally 2 and 6 kHz.

facilitated by imagining Fig. 2 to be rotated counterclockwise through 90° and relating it to Fig. 1(b), using the points labeled P_1 and P_2 in the two figures as reference points. This comparison verifies two important features predicted by the following analysis: (1) The derivative $d\omega/d\Omega$ goes from positive to negative at two frequencies (P_1, P_2) which are close to, but separated by, $\Omega_{LH}/2\pi$. (2) $d\omega/d\Omega$ goes from negative to positive at a frequency slightly higher than $\Omega_{LH}/2\pi$. The frequency separation between P_1 and P_2 in Fig. 2 is 1.1 MHz. This value can be compared with the theoretical value, which is obtained from Eq. (4) as $(\omega_*/2\pi)/(k\lambda_D)^2$. Using $\omega_*/2\pi$ from Fig. 2 with the values of k and λ_D as estimated above, we find the theoretical value to be 2.4 MHz. In view of the approximate nature of the estimated quantities and the fact that there may be other factors not included in the theory, this result is regarded as satisfactory at this preliminary stage.

The details of the damping of the drift wave in the region $\Omega > \Omega_{LH}$ as obtained in separate experiments are shown in Fig. 3. Although the amplitude of the exciting signal to the coil is kept constant in this series, the rf electric field in the plasma follows the resonance response of the lower-hybrid mode, being reduced by about 30% for $\Omega/2\pi = 2.70$ MHz. It is noted that the drift-wave amplitude is reduced dramatically for relatively small changes in the applied frequency Ω and the drift frequency ω. [Typically, the amplitude is reduced by at least 10 dB (power) with a 10% change in ω.] This feature is consistent with the rapid frequency dependence of electron Landau damping, as discussed above. It should also be noted that the onset of strong damping does not occur when $\Omega = \Omega_{LH}$, but at a frequency somewhat higher than Ω_{LH}, as might be expected because of the presence of the intermediate region labeled "2" in Fig. 1(c).

The theory[5] predicts that the method described in this Letter can also be used to stabilize the drift-cyclotron loss-cone instability, which is of interest in mirror machines.[12] Finally, it is noted that the present method is related to a technique known as "dither" stabilization in control engineering. Dither stabilization is defined as the modification of the low-frequency properties of an unstable nonlinear system by the application of a high-frequency signal in order to stabilize the system.[13]

This work has been supported by National Science Foundation Grant No. ENG-76-04635 and by the U. S. Air Force Office of Scientific Research, Grant No. 76-3129.

[1]T. Consoli, IEEE Trans. Plasma Sci. 4, 257 (1976).

[2]Ya. B. Fainberg and V. D. Shapiro, Pis'ma Zh. Eksp. Teor. Fiz. 4, 32 (1966) [JETP Lett. 4, 20 (1967)].

[3]Ya. B. Fainberg and B. D. Shapiro, Zh. Eksp. Teor. Fiz. 52, 293 (1966) [Sov. Phys. JETP 25, 189 (1967)].

[4]M. Okamoto, T. Amano, and K. Kitao, J. Phys. Soc. Jpn. 29, 1041 (1970).

[5]A. K. Sundaram and P. K. Kaw, Nucl. Fusion 13, 901 (1973).

[6]G. Schmidt, in *Proceedings of the Third International Conference on Theoretical and Experimental Aspects of Heating Toroidal Plasmas, Grenoble, France, 1976* (Commissariat à l'Energie Atomique, Grenoble, France, 1976), Vol. 2, p. 239.

[7]Although the analysis of Ref. 3 assumes a uniform pump field ($K_z/K = 0$), it is used here since $K_z/K \ll 1$ for the present experimental geometry. Thus, we take $K_z/K \neq 0$ in Eq. (1), as explained later in the text, but assume $K_z/K = 0$ otherwise. As is shown by the experimental results, this procedure only causes a quantitative modification of the theoretical coupling between the longitudinal components of the drift and lower-hybrid waves.

[8]A. A. Galeev, V. N. Oraevskii, and R. Z. Sagdeev, Zh. Eksp. Teor. Fiz. 44, 903 (1963) [Sov. Phys. JETP 17, 615 (1963)].

[9]R. Gore, H. Lashinsky and J. R. Conrad, Bull. Am. Phys. Soc. 21, 1075 (1976).

[10]R. Gore, Ph.D. thesis, Institute for Physical Science and Technology, University of Maryland, 1977 (unpublished); R. Gore and H. Lashinsky, to be published.

[11]H. Lashinsky and R. E. Monblatt, Rev. Sci. Instrum. 42, 1413 (1971).

[12]D. E. Baldwin, Rev. Mod. Phys. 49, 317 (1977).

[13]A. Gelb and W. E. Vander Velde, *Multiple-Input Describing Functions and Nonlinear System Design* (McGraw-Hill, New York, 1968).

Influence of Internal Fields on Magnetic and Electric Orientational Effects in Superfluid ^{3}He

I. A. Fomin
L. D. Landau Institute of Theoretical Physics, U.S.S.R. Academy of Sciences, Moscow, U.S.S.R.

and

C. J. Pethick
Department of Physics, University of Illinois at Urbana-Champaign, Urbana, Illinois 61801, and NORDITA, DK2100 Copenhagen Ø, Denmark

and

J. W. Serene
Department of Physics, State University of New York, Stony Brook, New York 11794

(Received 3 February 1978)

We examine how internal fields affect orientational energies in superfluid ^{3}He. We find that the orientational effect of a magnetic field due to the interaction between magnetic dipole moments is increased modestly, but that the analogous effect due to the interaction between electric dipole moments induced by an external electric field is suppressed significantly. Our estimated of the electric fields required to produce orientational effects are at least an order of magnitude larger than previous ones.

In superfluid ^{3}He the interaction between magnetic dipole moments gives rise to an energy which tends to orient the spin part of the order parameter relative to the orbital part. The dipolar coupling parameter, g_D, cannot be calculated precisely because it depends on unknown frequency and momentum dependences of the energy gap for frequencies of order ϵ_F and for momenta far from the Fermi surface, which serve to cut off logarithmically divergent sums. In the usual BCS model these dependences are simulated by a simple step-function cutoff in momentum. In this case, the theoretical values for g_D are consistent with experimental determinations for reasonable values of the cutoff, if one neglects internal-field effects.[1] Takagi[2] has estimated the effects of internal fields using the paramagnon model, and he too finds agreement between theory and experiment for a physically reasonable value of the cutoff. As first pointed out by Delrieu,[3] one expects the interaction between induced electric-dipole moments to produce an analogous energy which tends to orient the orbital part of the order parameter relative to an electric field. Whereas the magnetic orientational effect has been well verified experimentally, the electric orientational

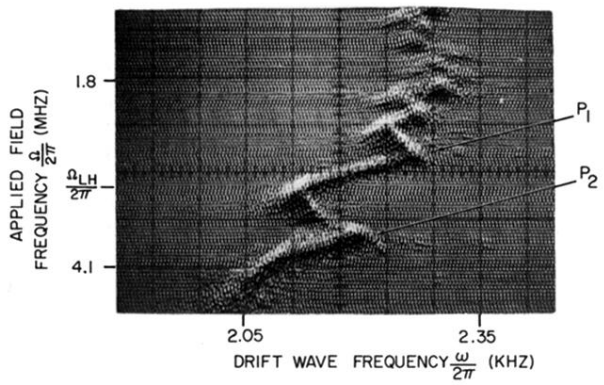

FIG. 2. The dependence of drift-wave frequency $\omega/2\pi$ on applied frequency $\Omega/2\pi$ as shown by a raster display (Ref. 11). In this display system successive sweeps of a spectrum analyzer are stacked one above the other. The points marked $P_1 = 2.6$ MHz and $P_2 = 3.7$ MHz are to be compared with similarly designated points in Fig. 1(b). The secular frequency shift is due to a variation in rf power coupled into plasma caused by the frequency dependence of the coil Q and by the distributed capacity of the coil.